Jurnal Kejuruteraan 33(2) 2021: 239-248
https://doi.org/10.17576/jkukm-2021-33(2)-09

Computational Fluid Dynamics Simulation of Fluidized Bed Dryer for Sago Pith Waste Drying Process.

Abdul Mu'im Abdul Nasir[a], Masli Irwan Rosli[a*], Mohd Sobri Takriff[a], Nur Tantiyani Ali Othman[a] & Vinotharan Ravichandar[b]
[a]*Research Centre for Sustainable Process Technology (CESPRO),*
[b]*Chemical Engineering Program,*
Faculty of Engineering & Built Environment, Universiti Kebangsaan Malaysia, Malaysia

**Corresponding author: masli@ukm.edu.my*

Received 18 April 2020, Received in revised form 11 September 2020
Accepted 01 October 2020, Available online 30 May 2021

ABSTRACT

Sago pith waste (SPW) has a great potential in becoming numerous kinds of reusable products as it has high level of starch content after went through drying process. Without proper treatment the disposal of SPW could cause serious environmental problem. The drying process of SPW using fluidized bed dryer (FBD) was found to be more effective than other drying methods. Thus, in this study the process was analyzed using computational fluid dynamics (CFD) modelling with the developed three-dimensional FBD model. The fluidization profile was studied from the analysis done using ANSYS Fluent 19.2 software which include certain process flow and set up to create similar situation as the experimental condition by also taking into account the moisture content of SPW. Both approach of drying process were executed at air inlet temperature of 50°C and velocity at 1.50 ms^{-1}. Using the sample of SPW that initially at 40% wet basis the result of fluidization from experimental and simulation were comparable in term of particles profiles and percentage of moisture content which show closely resemblance of decreasing trend. The outcome was however having a slight different of moisture content at 15th minute of experimental approach which could be resolved by improving the model in term of zone condition of the simulation setup. This study is however is an initial part to study about SPW drying using CFD solution as there are more to be discovered with this advantageous tool that is able to perform and provide much more analysis and outcomes in much shorter time and cost saving way base on the experimental method.

Keywords: Computational Fluid Dynamics (CFD), Drying; Sago pith waste; Fluidized Bed Dryer (FBD)

INTRODUCTION

Sago pith waste (SPW), known as sago fibrous residue, is produced from the extraction of sago starch from the sago palm rasped pith (Lai et al. 2013). The pith of sago can be found at the inner part of the trunk after the outer bark-like layer is removed. Sago starch cumulates in the sago palm pith stem from the base upward. A mature trunk is fully flooded with starch almost to the crown (Pei-Lang et al. 2006). A study was done to investigate the characteristics of SPW which could be summarized in Table 1.

Malaysia is known it is known to be the world's largest exporter of sago products despite only about more than 60,000 hectares of sago planting area, due to the advance in sago processing technology (Mohamad Naim et al. 2016). Compare to the neighboring country which is Indonesia (2,942,278 ha) and Papua New Guinea (1,020,000 ha), Malaysia took the third place in term of planting area of sago which specifically found in Mukah division under the state of Sarawak that include 59,000 hectares (Ahmad 2014).

Approximately 50–110 ton of sago pith is produced daily in Sarawak, especially in Sibu and Mukah Districts. Almost 66% starch and 14% fiber on a dry weight basis are contained in the pith, where about 25% consists of lignin (Awg-Adeni et al. 2010). Linggang et al. (Linggang et al. 2012) reported that raw sago pith residue consists of 58% starch, 23% cellulose, 9.2% hemicellulose and 3.9% lignin on a dry weight basis.

It has been found by numerous researchers the huge potential of SPW that are able to be commercialized. Previous works have reported the function of SPW as feed for the animal farming industry. SPW is used as swine feed because it contains substantial starch residue inside the pith (Awg-Adeni et al. 2010). The same research also found that SPW is suitable to be consumed by ruminants because the value of SPW feeding is closely similar to sweet potato residues. SPW can also be used as animal feed in the form of spirulina biomass (Phang et al. 2000).

A previous study found that SPW could be plasticized into a biodegradable composite material without additional synthetic plastic as binder because it contains high percentage of starch (Lai et al. 2013). The SPW starch has been successfully converted to fermentable sugar that can be treated further via microbial fermentation to produce ethanol (Pang et al. 2018). One study discovered that

TABLE 1. SPW properties (Lai et al. 2013)

Properties	Condition
Moisture content	82%
Circle equivalent (CE) diameter	44.82 µm
Starch content	58 – 67%
Degradation temperature	220ºC
Major components	Hemicellulose, cellulose and lignin

FIGURE 1. Sago palm tree.

bioethanol could be produced from glucose recovered from the residual starch of SPW (Awg-Adeni et al. 2013).

It is crucial to come out with an effective way to process the residue of processed sago as the industry of this crop is growing and going to be expanded throughout the time. Otherwise the environment will get effected by the normal practice of disposing SPW to the river. In addition by enhancing the method of SPW drying, it could encourage the development of SPW useful products. Drying is the effective further treatment of SPW as it could remove the moisture from it by evaporating its moisture content (Mohd Noh et al. 2018).

Fluidized drying has been widely used in industry and fluidized bed dryer (FBD) is a well-known dryer used for wet solid particle drying. Researches in drying of material in FBD have been done either from experimental or simulation and it been used including for cylindrical carrot (Tatemoto et al. 2016), food grain (Azmir et al. 2018), soybean meal (Da Silva et al. 2012), coconut residue (Assawarachan 2013), bird's chillies (Tasirin et al. 2007), bean (Nitz & Taranto 2007), pepper (Chuwattanakul & Eiamsa-Ard 2019), apple cubes (Galvão et al. 2019), sago pith waste (Rosli et al. 2020) and kaffir lime (Tasirin et al. 2014). All of these products have been effectively dried using FBD.

FBD has several advantages which include providing large contact area between solid and air, high solid mixing level and high heat and moisture transfer coefficient between solid and air (Mortier et al. 2011). In addition, it gives a better temperature and operation control along the drying process. Process temperature is able to be maintained for an optimum drying. Other than that it involve low maintenance cost due to no moving part involve (Antony & Shyamkumar 2016). FBD also offers significant advantages like uniform moisture reduction with less drying time and high drying rate (Kassem et al. 2011) compared to others drying method. Another essential advantage of FBD is the ability to control temperature well that made heat sensitive materials drying become effective such as pharmaceutical or food products (Alaathar et al. 2013). All of these factors have made FBD as a favourable medium to complete the drying process task.

CFD-based techniques are used to study and solve complex engineering applications, including fluid flow and heat and mass transfer problems (Jamaleddine & Ray 2010). CFD is a simulation instrument that utilises high-performance computers and applied mathematics to simulate fluid flow conditions and help design industrial processes optimally (Anandharamakrishnan 2010). Previous studies have shown that CFD is a useful tool for predicting gas and particle flow pattern, such as velocity, time residency and impact position (Anandharamakrishnan 2010).

Numerous studies have explained the application of CFD in the drying process. A recent research investigated the drying conditions of SPW in FBD using CFD modelling from Ansys Fluent package (Rosli et al. 2018). The study focused on the suitable drying condition of SPW in terms of particle size and drying air velocity. A study that has been done by Tantiyani Ali Othman & Elmi Fahmi Mohd Razali (2019) has also successfully comprehended the factors that influenced the quality of coffee production by applying the same CFD technique. Smolka et al. investigated the heat and flow process inside a drying oven using 3D modelling

analysis to improve the temperature uniformity (Smolka et al. 2010).

CFD has been consumed progressively to enhance process design capabilities in numerous industrial applications and drying processes. Recent developments in mathematical techniques and computer hardware have helped CFD to predict the drying phenomenon in different types of industrial dryer. All types of drying operation have been utilised, including freezing, spraying and thermal drying techniques. CFD-based methods are also already being used in designing and evaluating commercial dryers for the pharmaceutical, food, chemical, mining, agricultural and petroleum industries (Jamaleddine & Ray 2010).

Thus in this research the objective is to determine the fluidization profile of SPW drying process. It is also an aim of this study to find out the moisture content of SPW at stated condition of drying.

METHODOLOGY

INTRODUCTION

This study was done by using two kinds of approaches which is analyzing the fluidization of SPW using CFD software, ANSYS 19.2 (ANSYS Inc., version 19.2, Canonsburg, PA, USA) under Fluent package assisted by a computer that equipped with Windows 8 64-bit operating system, Intel Core i5 processor, and 8.00 GB RAM. The result from the simulation was then validated with the experimental approach using a lab scale FBD (Figure 2). In order to validate the simulation results of fluidization profile and moisture content of SPW, the air inlet temperature and velocity were set as the parameters as these parameters are the main operating conditions in FBD to determine the SPW drying process performance.

EXPERIMENTAL DRYING

90% wet basis of SPW sample (Figure 3) which was obtained from the mill (Hup Moh Kilang Tepong Sago, Batu Pahat, Johor, Malaysia). To prepare SPW sample at desired moisture content, fully-dried SPW was re-wetted using distilled water to obtain the desired moisture content. The amount of water that needed to be added was determined using the moisture content equation (Touil et al. 2014):

$$X_t = \frac{m_o - m_d}{m_o} \quad (1)$$

where:

m_o = mass of original sample,
m_d = mass of dried sample

The desired air temperature and velocity in the fluidized bed dryer is at 50°C and 1.50 ms^{-1}. Initially, the FBD was run with hot air for 15 minutes. To inspect the air temperature and velocity inside the dryer is in the desired range, anemometer was used before the drying experiment was carried out. Once the dryer is run, the Hold button on the anemometer was pressed to stop further value changes. After the air temperature and velocity reaches the desired

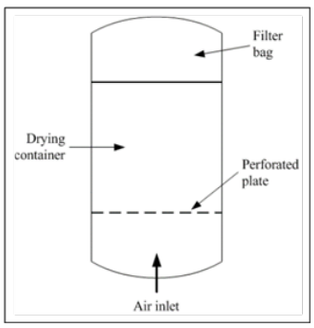

FIGURE 2. Diagram of lab scale FBD.

FIGURE 3. Sample of SPW.

value, SPW sample was placed into the dryer. SPW was weighed for every 5 minutes using the analytical balance. Drying using fluidized bed dryer was carried out until it reaches 0% wet basis.

COMPUTATIONAL FLUID DYNAMIC (CFD) SIMULATION

Generally, steps in doing analysis using ANSYS shown in figure 4. Starting with geometry process the drawing of the equipment to be use in SPW drying, FBD was done in ANSYS SpaceClaim 19.2 (ANSYS Inc., version 19.2, Canonsburg, PA, USA) with similar dimension and design with the lab scale FBD model Fluid Bed Dryer TG 200 (Retsch GmbH, Haan, Germany) in three dimensional (3D) form. The FBD has the high of 520mm (include the filter bag) and diameter of 220mm.

Followed by meshing process; the size of element, type of meshing, sizing, and quality of meshing was done to get an accurate result of simulation. To obtain good quality of meshing, a mesh independency test was done. The boundary was also set at this point which include inlet, outlet, and wall boundary. Table 2 shows in short the setup of meshing process for the 3D model of FBD use for the simulation process.

There are several assumptions have been made before the simulation take place:

1. Particle size is fixed at 200µm to obtained good fluidization (Rosli et al. 2018)
2. Chemical reaction does not occur in the drying process.
3. Gas and solid are well-mixed.
4. Slip conditions are not set.
5. Initial moisture content of SPW is 40% which is meet the appropriate moisture content range in FBD.
6. SPW does not accumulate at a moisture content of 60%.
7. Final moisture content of SPW expected to achieve 10% to prevent from SPW's nutrient depletion (Babu et al. 2018).
8. Particle size is not reduced with drying time and the different particle sizes are classified based on Geldart theory.
9. The thermal properties of SPW are represented by the properties of cassava (Lamidi et al. 2019; Rosli et al. 2018).

The simulation in this study was performed for the transient time-dependent. The next step is to choose the physic mode that suitable with the study. Models selection, material boundary conditions, material designation, solution methods and parameter involved in this study was assigned in this level.

To ensure that minimum computational effort will be use in this study the Eulerian-Eulerian multiphase model has been chosen to carry out the simulation with three Eulerian phases consist of fluid, solid and mixture. This model has been commonly applied on others CFD modelling of FBD. The standard k-epsilon model was also chosen as it requires minimum computational effort and easiness. To analyze heat transfer of the phases in the model the heat transfer or energy model was also activated.

The main equations that are considered as essential in the multiphase model are conservation of mass, momentum and energy. In the case of heat transfer and turbulence flow, energy conservation and turbulence model are also take into consideration (Argyropoulos & Markatos 2015).

Conservation of mass ("17.5.4. Conservation Equations" 2019):

$$\frac{\partial}{\partial t}\left(\alpha_q \rho_q\right)+\nabla\cdot\left(\alpha_q \rho_q \vec{v}_q\right)=\sum_{p=1}^{n}\left(\dot{m}_{pq}-\dot{m}_{qp}\right)+Sq \quad (2)$$

Where:

$\vec{v}_q$ = represent velocity for q phase;
n_{pq} = mass transfer from pth phase to qth phase;
n_{qp} = mass transfer from qth phase to pth phase.

Conservation of Momentum ("17.5.4. Conservation Equations" 2019):

$$\frac{\partial}{\partial t}\left(\alpha_q \rho_q \vec{v}_q\right)+\nabla\cdot\left(\alpha_q \rho_q \vec{v}_q \vec{v}_q\right)= -\alpha_q \nabla p+\nabla\cdot\bar{\bar{\tau}}_q+\alpha_q \rho_q \vec{g}+\sum_{p=1}^{n}(\vec{R}_{pq}+\dot{m}_{pq}\vec{v}_{pq}-\dot{m}_{qp}\vec{v}_{qp})+\left(\vec{F}_q+\vec{F}_{lift,q}+\vec{F}_{wl,q}+\vec{F}_{vm,q}+\vec{F}_{td,q}\right) \quad (3)$$

$$\bar{\bar{\tau}}_q=\alpha_q \mu_q\left(\nabla\vec{v}_q+\nabla\vec{v}_q^{T}\right)+\alpha_q\left(\lambda_q-\frac{2}{3}\mu_q\right)\nabla\cdot\vec{v}_q\,\bar{\bar{I}} \quad (4)$$

where:

τ_q = qth phase shear stress tensor
$_q$ = shear viscosity of phase q;
λq = bulk viscosity of phase q;
$\vec{F}_q$ = external body forces;
$\vec{F}_{lift,q}$ = lift forces;
$\vec{F}_{wl,q}$ = wall lubrication forces;
$\vec{F}_{td,q}$ = virtual mass and turbulent dispersion forces;
R_{pq} = interaction force between phases;
p = pressure shared by all phases.

Conservation of Energy:

$$\frac{\partial}{\partial t}\left(\alpha_q \rho_q h_q\right)+\nabla.\left(\alpha_q \rho_q \vec{u}_q h_q\right)= \alpha_q\frac{\partial p_q}{\partial t}+\bar{\bar{\tau}}_q:\nabla\vec{u}_q-\nabla.\vec{q}_q+S_q+\sum_{p=1}^{n}\left(Q_{pq}+\dot{m}_{pq}h_{pq}-\dot{m}_{qp}h_{qp}\right) \quad (5)$$

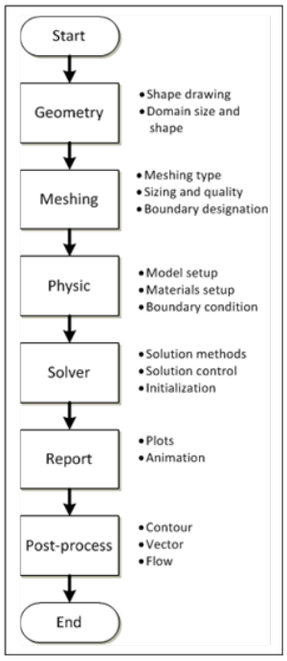

FIGURE 4. ANSYS Fluent simulation process.

where:

h_q = specific enthalpy of the qth phase;
$\vec{q}_q$ = heat flux;
S_q = source of enthalpy;
Q_{pq} = intensity of heat exchange between the pth and qth phases
h_{pq} = interphase enthalpy

Transport Equation ("17.5.4. Conservation Equations" 2019):

$$\frac{\partial}{\partial t}(\rho k)+\frac{\partial}{\partial x_i}(\rho k u_i)= \frac{\partial}{\partial x_j}\left[\left(u+\frac{u_t}{\sigma_k}\right)\frac{\partial k}{\partial x_j}\right]+ G_k+G_b-\rho\dot{o}-Y_M+S_k \quad (6)$$

$$\frac{\partial}{\partial t}(\rho\dot{o})+\frac{\partial}{\partial x_i}(\rho\dot{o}u_i)= \frac{\partial}{\partial x_j}\left[\left(u+\frac{u_t}{\sigma_{\dot{o}}}\right)\frac{\partial\dot{o}}{\partial x_j}\right]C_{1\dot{o}}\frac{\dot{o}}{k} \left(G_k+C_{3\dot{o}}G_b\right)-C_{2\dot{o}}\rho\frac{\dot{o}^2}{k}+S_{\dot{o}} \quad (7)$$

where:

G_k = generation of turbulence kinetic energy due to mean velocity gradients;
G_b = generation of turbulence kinetic energy due to buoyancy;
Y_M = contribution of the fluctuating dilatation in compressible turbulence to the overall rate;
$C_{1\dot{o}}$, $C_{2\dot{o}}$ and $C_{3\dot{o}}$ = constants;
$S_{\dot{o}}$, S_k = user source term.

Model Two-Term Exponential:

$$MR = aexp(-kt) + (1-a)exp(-kat) \quad (8)$$

$$k = 4.882\times10^{-4}T + 1.506\times10^{-3}v - 2.23\times10^{-3} \quad (9)$$

where;

MR = moisture ratio;
k = drying constant;
T = air temperature;
v = air velocity;
t = drying time (min);
a = constant = 2.0888 (Ho. Y.N. 2016)

After all the models was identified, materials and also their properties that involved in the drying process was introduced into the simulation that include sago particle, nitrogen (N_2), oxygen (O_2), water vapor (H_2O vapor) and water liquid (H_2O liquid). Then boundary condition of the simulation was determined that similar to the experimental setup. For better understanding of the simulation Table 3 shows the details of setting used in ANSYS Fluent in this study and the selected modules that appropriate with the study parameter to simulate the drying of SPW in FBD.

The simulation was executed after all the setup was done and the result was evaluated using CFD-Post software. This software is able to provide various form of result such as contour, flow, plot, vector and animation. The observation of the SPW was done onto its flow profile to compare with the profile generated from the experimental procedure. This was done to find out the similarity of both approaches taken which will determine

TABLE 2. Meshing process setting

Details	Option		
Default	Physics Preference		CFD
	Solver Preference		Fluent
	Element Order		Linear
	Element size		1.3e-002m
	Export Format		Standard
Sizing	Use Adaptive Sizing (No)	Growth rate	1.2
		Max Size	2.6e-002 m
	Mesh Defeaturing (Yes)	Defeature Size	6.5e-005 m
	Capture Curvature (Yes)	Curvature Min Size	1.3e-004 m
		Curvature Normal Angle	18.0º
	Capture Proximity		No
Face sizing	Scope	Scoping Method	Geometry Selection
	Definition	Suppressed	No
		Type	Element size
	Advanced	Defeature Size	Default
		Behavior	Soft
		Capture Curvature	No
		Capture Proximity	No
Inflation	Scope	Scoping Method	Geometry Selection
	Definition	Suppressed	No
		Boundary Scoping Method	Geometry Selection
		Inflation Option	Smooth Transition
		Inflation Algorithm	Pre
Body Sizing	Scope	Scoping Method	Geometry Selection
	Definition	Suppressed	No
		Type	Element size
	Advanced	Defeature Size	Default
		Behavior	Soft
		Capture Curvature	No
		Capture Proximity	No

either the computational process of drying could represent the experimental drying of SPW. In order to evaluate the result from CFD-Post, SPW flow profile was observed at the middle cut of the FBD XY plane.

The result obtained from both experimental and computational method will then being compared to analyze the fluidization profile of SPW in each approach. The visual evaluation is one of a method to determine either the computational approach could represent the experimental method.

RESULTS AND DISCUSSION

INTRODUCTION

The outcome from both experimental and simulation procedure has been done and in this section the findings will be discussed which mainly focused on the visual observation of particle profiles and percentage of moisture content in SPW.

EXPERIMENTAL OUTCOME

The drying process of SPW was done using a lab scale FBD at temperature of 50ºC and 1.5 ms^{-1} of air velocity at the inlet. Fluidization profile from the process was generated as shown in figure 5.

The moisture content of SPW sample was set at 40% wet basis at the beginning of drying process. The SPW will only fluidize if it reaches a good flow character which is at 10% wet basis. Referring to figure 5, at the beginning of the drying process (0 min), the SPW bed was still at a fixed bed layer. When the SPW reaches a good flow, the bubbling fluidization can be observed increasingly on the sago surface (5 to 10 min). Bubbling fluidization occurred infrequently on the SPW layer (15 min). After moisture

TABLE 3. ANSYS Fluent setup condition

Setting mode	Panel selection		Description
General	Solver	Type	Pressure-based
		Time	Transient
	Gravity	9.81 ms^{-2}	
Models	Multiphase (Eulerian)	Phases	Phase 1 - Air Phase 2 - Sago Phase 3 – Water vapor
		Particle size	2000 μm
		Phase interaction	Mass transfer mechanism – evaporation condensation Sago (H_2O liquid) to H_2O (vapor)
	Viscous	k-epsilon	Realizable
		Near-wall treatment	Scalable Wall Functions
		Turbulence Multiphase Model	Dispersed
	Species (Transport)	Phase	H_2O vapor
Materials	Fluid		Air, N_2, O_2, Sago particle, H_2O (liquid), H_2O (vapor)
	Mixture		Air – O_2, N_2, H_2O (vapor)
			Sago – H2O (liquid), Sago particle
Boundary condition	Inlet		Air velocity = 1.5 ms^{-1}
			Air temperature = 50 ℃
			Pressure = 101325 Pa
Solution	Methods	Scheme	Phase Coupled SIMPLE
		Transient Formulation	First Order Implicit
	Initial moisture content		Sago = 40% Water Liquid = 60%
Calculation	Time step size		0.01
	Number of time steps		500

content reached 0% wet basis, turbulent fluidization was achieved and the drying process is considered completed after 20 minute.

Figure 6 shows the graph of moisture content of SPW from experimental and simulation. Generally the graph showed that SPW's moisture continuously decreasing with drying time for both study approaches. However there is a slight fluctuation of simulation result at time 15 minute compared to the experimental. This might be caused by unequal particle size and shape of SPW that is significantly varied as agreed by a research done by Román et al. (2012). Another rationale contributing to this outcome is there were dissimilarities process characteristics of SPW between the real SPW and assumptions made for simulation (F. D. Román & Hensel 2014).

Even though the final moisture content achieved via simulation (4.0%) was quite deviated with the experimental (0.04%) it is still under acceptable range of desired final moisture content of SPW which is 10%.

CFD SIMULATION OUTCOME

The geometry drawing of FBD was done using ANSYS SpaceClaim that have a cylindrical shape as shown in Figure 7.

A mesh independency test was done based on the temperature at the model outlet. The test was done from five different cell number ranged from 600 cells number to 80,000 cells number as stated in Table 2. Based on figure 8, the temperature different between cell number 53,843, 82129, and 88,258 show differentiation of outlet air temperature less than 5% from each other. Thus, the cell number of 82,129 was chosen to perform the simulation for SPW drying in CFD Fluent. Figure 9 show the mesh structure of the FBD model that consist of 20,611 nodes and 83,084 number of elements or cells.

The simulation method was done using the developed 3D model of FBD for SPW drying process. The model was validated based on the experimental procedure. The parameter involved which is air inlet velocity was set at 1.50 ms^{-1} and air inlet temperature at 50ºC with particle size of 200µm. Accomplished simulation was then being analyzed using ANSYS CFD-Post to obtain the fluidization profile of SPW volume fraction that indicate SPW behavior along the drying process inside FBD drying chamber. The result of SPW particles profiles was observed at the XY plane of the model. As shown in figure 5, the simulation was occurred within 5 second that could portray the experimental method that took about 20 minutes.

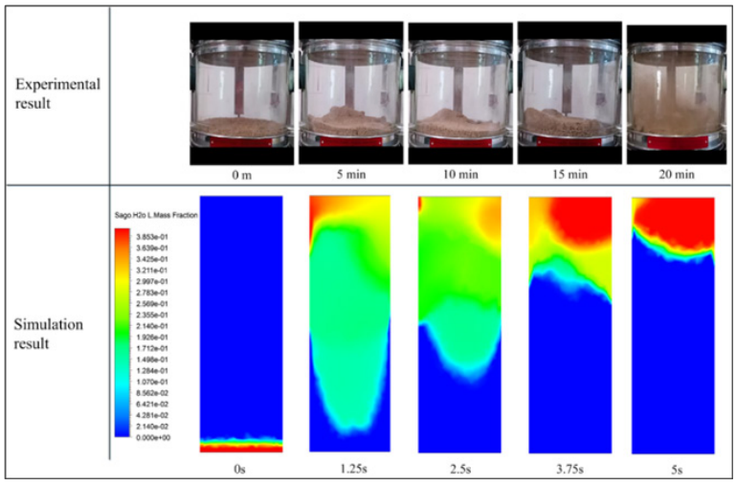

FIGURE 5. Visual comparison of experimental and simulation result on SPW particle profiles.

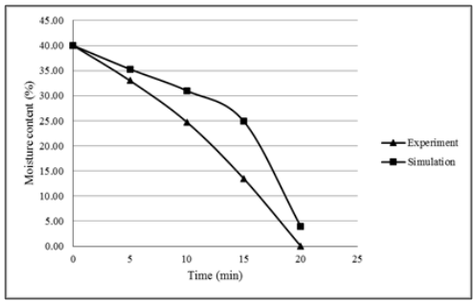

FIGURE 6. Moisture content of SPW from experiment and simulation.

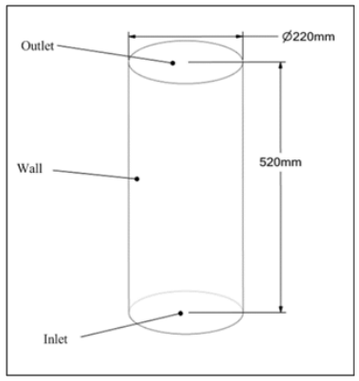

FIGURE 7. Three-dimensional drawing of FBD.

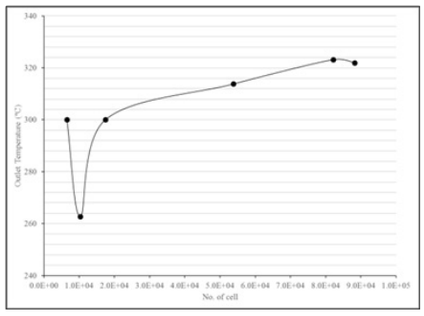

FIGURE 8. Graph of mesh independency test result.

FIGURE 9. Mesh structure of 3D FBD model.

The SPW mostly started to leave the original bed height and moving up along the drying chamber at the first second of the process. At the time of 1.25s, the bubbling fluidization started to occur until the end of the simulation.

The final profile of SPW fluidization indicate that SPW has the maximum moisture content of 4% (figure 3). Another similar study has been done previously on SPW using same simulation method done by Masli et al. (Rosli et al. 2018). The inlet air was set at the same temperature, but the velocity was set at 1.30 ms^{-1} with same size of particle which is 2000 µm. Different profile of fluidization was shown between the results obtained from both studies as that research indicate minimal bed expansion of bubbling fluidization was take place and it

was unable to reach the maximum size and falling back to the original bed height.

EXPERIMENTAL AND COMPUTATIONAL COMPARISON

Both experimental and simulation result obtained were compared in term of fluidization profile and also the moisture content. This step was taken to find out if the simulation approach is reliable to represent the experimental method of SPW drying process.

As shown in Figure 2, the fluidization of SPW volume fraction from the simulation shows quite similar profile compare to the outcome from the experiment especially at the last phase of the process. The fluidization behavior from the experimental at the time of 15min show comparable result with the simulation result at time of 4s which picturized the SPW begin to fluidize. The final stage of drying process from experimental at 20 min shown the indistinguishable fluidization profile compare to the last period of simulation procedure at 5s as SPW has filled most the dryer chamber.

Generally, both experimental and simulation approach showed continuously decreasing percentage of SPW moisture content over time. However, the moisture content of SPW from simulation show slight difference value compared to the experiment especially at time 15 min (3.75s simulation). This difference could be overcome by revising the model used and improving the zone condition of 3D model in the simulation setup.

CONCLUSION

Two ways of SPW drying process approaches have been done in this study to visually investigate the fluidization profile produced in term of volume fraction. The drying experiment was done using lab scale FBD to dry 90% wet basis of SPW with 1.50 ms^{-1} and 50ºC of air inlet. The procedure took 20 minutes for the SPW to reaches 0% of moisture content.

Using same condition representing the experimental method, a simulation using a validated 3D model was done to perform the drying of SPW. With the application of Eulerian multiphase model and other related models available in the software used, a fluidization profile was managed to be generated and minimized the moisture content of SPW at the completion of the drying process. The simulation result obtained also being matched with the research done by Masli et al. (Rosli et al. 2018).

The experimental and simulation outcome was being compared to find the similarity on the fluidization profile and percentage of moisture content. It was showed that the fluidization profile of SPW from experimental at time 15min and 20min were comparable to the simulation mainly at the last phase of the fluidization which is at time 3.75s and 5s. Water removal from both method also show similar increasing trend through time.

From this finding it could be assume that the simulation approach is reliable to execute the drying process of SPW with further enhancement to take place. More specific analysis is vital to be done as CFD tool offers various kind of information related to the fluidization process which include fundamental parameter analysis such as pressure, velocity and temperature; moisture content and drying rate. This precise analysis are quite limited to be reached and involves time consuming through the experimental procedure but it become possible with the help of the computational method with the right knowledge and application technique.

ACKNOWLEDGEMENT

The authors would like to acknowledge Universiti Kebangsaan Malaysia and the Ministry of Higher Education, Malaysia for supporting this project under research grant FRGS/1/2017/TK02/UKM/02/5.

DECLARATION OF COMPETING INTEREST

None.

REFERENCES

17.5.4. Conservation Equations. 2019. https://www.sharcnet.ca/Software/Ansys/17.0/en-us/help/flu_th/flu_th_sec_eulermp_theory_conseq.html [16 July 2019].

Ahmad, M. 2014. Farmer empowerment to increase productivity of sago (metroxylon sago spp) Farming. *International Journal on Advanced Science, Engineering and Information Technology* 4(3): 129.

Alaathar, I., Hartge, E. U., Heinrich, S. & Werther, J. 2013. Modeling and flowsheet simulation of continuous fluidized bed dryers. *Powder Technology* 238: 132–141.

Anandharamakrishnan, C. 2010. Computational fluid dynamics (CFD) applications in spray drying of food products. *Trends in Food Science & Technology* 21(8): 383–398.

Antony, J. & Shyamkumar, M. B. 2016. Study on Sand Particles Drying in a Fluidized Bed Dryer using CFD. *International Journal of Engineering Studies* 8(2): 975–6469. Retrieved from http://www.ripublication.com

Argyropoulos, C. D. & Markatos, N. C. 2015. Recent advances on the numerical modelling of turbulent flows. *Applied Mathematical Modelling* 39(2): 693–732.

Assawarachan, R. 2013. Drying Kinetics of Coconut Residue in Fluidized Bed 2(2): 263–266.

Awg-Adeni, D. S., Abd-Aziz, S., Bujang, K. & Hassan, M. A. 2010. Bioconversion of sago residue into value added products. *African Journal of Biotechnology* 9(14): 2016–2021.

Awg-Adeni, D. S., Bujang, K. B., Hassan, M. A. & Abd-Aziz, S. 2013. Recovery of glucose from residual starch of sago hampas for bioethanol production. *BioMed Research International* 2013.

Azmir, J., Hou, Q. & Yu, A. 2018. Discrete particle simulation of food grain drying in a fluidised bed. *Powder Technology* 323: 238–249.

Babu, A. K., Kumaresan, G., Raj, V. A. A. & Velraj, R. 2018. Review of leaf drying: Mechanism and influencing parameters, drying methods, nutrient preservation, and mathematical models.

Renewable and Sustainable Energy Reviews 90(December 2016): 536–556.

Chuwattanakul, V. & Eiamsa-Ard, S. 2019. Hydrodynamics investigation of pepper drying in a swirling fluidized bed dryer with multiple-group twisted tape swirl generators. *Case Studies in Thermal Engineering* 13(January): 100389.

Da Silva, F. R. G. B., De Souza, M., Da Costa, A. M. de S., Jorge, L. M. de M. & Paraíso, P. R. 2012. Experimental and numerical analysis of soybean meal drying in fluidized bed. *Powder Technology* 229: 61–70.

Galvão, A. M. M. T., Rodrigues, S. & Fernandes, F. A. N. 2019. Kinetics of ultrasound pretreated apple cubes dried in fluidized bed dryer. *Drying Technology* 37(12): 1–11.

Ho. Y.N. 2016. *Pengoptimuman Proses Pengeringan Hampas Sagu di dalam Turus Terbendalir*. Universiti Kebangsaan Malaysia.

Jamaleddine, T. J. & Ray, M. B. 2010. Application of computational fluid dynamics for simulation of drying processes: A review. *Drying Technology* 28(2): 120–154.

Kassem, A. S., Shokr, A. Z., El-Mahdy, A. R., Aboukarima, A. M. & Hamed, E. Y. 2011. Comparison of drying characteristics of Thompson seedless grapes using combined microwave oven and hot air drying. *Journal of the Saudi Society of Agricultural Sciences* 10(1): 33–40.

Lai, J. C., Rahman, W. A. W. A. & Toh, W. Y. 2013. Characterisation of sago pith waste and its composites. *Industrial Crops and Products* 45: 319–326.

Lamidi, R. O., Jiang, L., Pathare, P. B., Wang, Y. D. & Roskilly, A. P. 2019. Recent advances in sustainable drying of agricultural produce: A review. *Applied Energy* 233–234(September 2018): 367–385.

Linggang, S., Phang, L. Y., Wasoh, M. H. & Abd-Aziz, S. 2012. Sago pith residue as an alternative cheap substrate for fermentable sugars production. *Applied Biochemistry and Biotechnology* 167(1): 122–131.

Mohamad Naim, H., Yaakub, A. N. & Awang Hamdan, D. A. 2016. Commercialization of Sago through Estate Plantation Scheme in Sarawak: The Way Forward. *International Journal of Agronomy* 2016: 1–6.

Mohd Noh, A., Mat, S. & Hafiz Ruslan, M. 2018. Development and Performance Analysis of New Solar Dryer with Continuous and Intermittent Ventilation (Pembangunan dan Analisa Prestasi Pengering Suria Baru dengan Mod Ventilasi Berterusan dan Bersela). *Jurnal Kejuruteraan 30 Special Issue* 1(3): 1–8.

Mortier, S. T. F. C., De Beer, T., Gernaey, K. V., Remon, J. P., Vervaet, C. & Nopens, I. 2011. Mechanistic modelling of fluidized bed drying processes of wet porous granules: A review. *European Journal of Pharmaceutics and Biopharmaceutics* 79(2): 205–225.

Nitz, M. & Taranto, O. P. 2007. Drying of beans in a pulsed fluid bed dryer: Drying kinetics, fluid-dynamic study and comparisons with conventional fluidization. *Journal of Food Engineering* 80(1): 249–256.

Pang, S. C., Voon, L. K. & Chin, S. F. 2018. Conversion of Sago (Metroxylon sagu) Pith Waste to Fermentable Sugars via a Facile Depolymerization Process. *Applied Biochemistry and Biotechnology* 184(4): 1142–1154.

Pei-Lang, A. T., Mohamed, A. M. D. & Karim, A. A. 2006. Sago starch and composition of associated components in palms of different growth stages. *Carbohydrate Polymers* 63(2): 283–286.

Phang, S., Miah, M. & Yeoh, B. 2000. Spirulina cultivation in digested sago starch factory wastewater. *Journal of Applied Phycology* 12: 395–400.

Román, F. D. & Hensel, O. 2014. Numerical simulations and experimental measurements on the distribution of air and drying of round hay bales. *Biosystems Engineering* 122: 1–15.

Román, F., Strahl-Schäfer, V. & Hensel, O. 2012. Improvement of air distribution in a fixed-bed dryer using computational fluid dynamics. *Biosystems Engineering* 112(4): 359–369.

Rosli, M. I., Abdul Nasir, A. M. & Ravichandar, V. 2020. Drying sago pith waste in a fluidized bed dryer. *Food and Bioproducts Processing*.

Rosli, M. I., Nasir, A. M. im A., Takriff, M. S. & Chern, L. P. 2018. Simulation of a fluidized bed dryer for the drying of sago waste. *Energies* 11(9): 2383.

Smolka, J., Nowak, A. J. & Rybarz, D. 2010. Improved 3-D temperature uniformity in a laboratory drying oven based on experimentally validated CFD computations. *Journal of Food Engineering* 97(3): 373–383.

Tantiyani Ali Othman, N. & Elmi Fahmi Mohd Razali, M. 2019. Drying of Instant Coffee in a Spray Dryer (Pengeringan Serbuk Kopi Segera dalam Pengering Sembur). *Jurnal Kejuruteraan* 31(2): 295–301.

Tasirin, S. M., Kamarudin, S. K., Jaafar, K. & Lee, K. F. 2007. The drying kinetics of bird's chillies in a fluidized bed dryer. *Journal of Food Engineering* 79(2): 695–705.

Tasirin, S. M., Puspasari, I., Lun, A. W., Chai, P. V. & Lee, W. T. 2014. Drying of kaffir lime leaves in a fluidized bed dryer with inert particles: Kinetics and quality determination. *Industrial Crops and Products* 61: 193–201.

Tatemoto, Y., Mibu, T., Yokoi, Y. & Hagimoto, A. 2016. Effect of freezing pretreatment on the drying characteristics and volume change of carrots immersed in a fluidized bed of inert particles under reduced pressure. *Journal of Food Engineering* 173: 150–157.

Touil, A., Chemkhi, S. & Zagrouba, F. 2014. Moisture diffusivity and shrinkage of fruit and cladode of opuntia ficus-indica during infrared drying. *Journal of Food Processing* 2014: 1–9.